Bulletin of Pure and Applied Sciences.
Vol.42 D (Physics), No.1,
January-June 2023 P. 70-78

Print version ISSN 0970 6569
Online version ISSN 2320 3218

Original Research Article

Available online at www.bpasjournals.com

Comparative Study of Wong's Formula and Coupled-Channel Models in Heavy-Ion Fusion: The ^16O+^144Sm Benchmark

Dr. Rahul Kumar[1]

Author's Affiliations:

Dr. Rahul Kumar [1]Assistant Professor (GT), Department of Physics, H.R. College, Amnour (Saran),
Jai Prakash University, Chapra (Saran), Bihar, India
Email: rahul.nishu@yahoo.com

***Corresponding author:** **Dr. Rahul Kumar**
Assistant Professor (GT), Department of Physics, H.R. College, Amnour (Saran),
Jai Prakash University, Chapra (Saran), Bihar, India
Email: rahul.nishu@yahoo.com

ABSTRACT Wong's analytical formula and the coupled-channels method represent the two ends of the spectrum of models used to describe heavy-ion fusion near the Coulomb barrier: the former reduces the problem to penetration of a single parabolic barrier, while the latter treats the coupling of the relative motion to the intrinsic excitations of the colliding nuclei to all orders. This article presents a systematic comparison of the two approaches, using the ^16O+^144Sm reaction as a benchmark. It is shown that the coupled-channels result can be cast, in the eigenbarrier representation, as a weighted sum of Wong-type cross sections over a distribution of barriers, which reduces exactly to Wong's formula when the couplings are switched off. The two models agree above the barrier, where both approach the classical geometric limit, but diverge by up to two orders of magnitude below it, where channel coupling generates the sub-barrier enhancement that the single-barrier formula cannot reproduce. The fusion barrier distribution sharply distinguishes the two: a single narrow peak for Wong's formula against a broad, structured profile for the coupled-channels calculation. The regime in which the simple formula remains adequate, and that in which the full treatment is indispensable, are delineated quantitatively

KEYWORDS Heavy-ion fusion, Wong's formula, Coupled channels, Barrier distribution, Sub-barrier enhancement, Eigenbarriers...

How to cite this article: Dr. Rahul Kumar. (2023). Comparative Study of Wong's Formula and Coupled-Channel Models in Heavy-Ion Fusion: The ^16O+^144Sm Benchmark Applied Sciences-Physics,42D (1), 64-69

INTRODUCTION

The fusion of two nuclei at energies near the Coulomb barrier is, in its simplest description, the penetration of a one-dimensional potential barrier formed by the competition between the long-range Coulomb repulsion and the short-range nuclear attraction [1, 2]. For a parabolic barrier this problem admits the elegant closed-form solution derived by Wong, which expresses the fusion cross section in terms of only three parameters: the barrier height, radius, and curvature [3]. For decades Wong's formula has served as the standard analytical tool for estimating fusion cross sections and for the rapid analysis of experimental excitation functions [4, 5].

It has, however, long been known that the single-barrier picture fails dramatically at sub-barrier energies, where measured fusion cross sections exceed its predictions by orders of magnitude [6, 7]. The resolution of this discrepancy lies in the coupling of the relative motion to the internal degrees of freedom of the colliding nuclei, in particular to their low-lying collective vibrations and rotations and to nucleon-transfer channels [8, 9, 10]. The coupled-channels method incorporates these couplings explicitly by solving a set of coupled radial equations, and it reproduces both the magnitude of the enhancement and the structure of the experimentally extracted barrier distribution [11, 12, 13].

The relationship between the two approaches is illuminated by the eigenbarrier, or barrier-distribution, representation [14, 15]. When the excitation energies of the coupled channels are small compared with the coupling strengths, the coupling matrix can be diagonalized at the barrier, and the coupled-channels cross section becomes an incoherent sum of single-barrier (Wong-type) cross sections, one for each eigenbarrier, weighted by the squared overlaps of the eigenchannels with the entrance channel. In this picture, Wong's formula is precisely the limit of the coupled-channels result in which all couplings vanish and the barrier distribution collapses to a single line.

This article presents a focused comparison of Wong's formula and the coupled-channels method. Section 2 develops both formalisms, the eigenbarrier representation that connects them, and the computational methodology. Section 3 compares the two models for the ^{16}O+^{144}Sm benchmark in terms of the excitation function, the barrier distribution, and the enhancement factor, and delineates their regimes of validity. Section 4 discusses limitations and future directions, and Section 5 summarizes the conclusions.

Notation: V_B, R_B, and $\hbar\omega$ denote the height, radius, and curvature of the uncoupled barrier; λ_α and w_α are the eigenbarrier shifts and weights; and E is the centre-of-mass energy.

2. Methods

2.1 The one-dimensional barrier and Wong's formula

For a single parabolic barrier of height V_B, radius R_B, and curvature $\hbar\omega$, the transmission coefficient for the l-th partial wave is given by the Hill–Wheeler expression,

$$T_l(E) = \left[1 + \exp\left(\frac{2\pi}{\hbar\omega}\left(V_B + \frac{\hbar^2 l(l+1)}{2\mu R_B^2} - E\right)\right)\right]^{-1}. \qquad (1)$$

Summing the partial-wave contributions to the fusion cross section,

$$\sigma_{fus}(E) = \frac{\pi}{k^2}\sum_{l=0}^{\infty}(2l+1)\,T_l(E), \qquad k^2 = \frac{2\mu E}{\hbar^2}, \qquad (2)$$

and approximating the sum by an integral under the assumption of an l-independent barrier radius and curvature, one obtains Wong's closed-form result,

$$\sigma_{fus}^{W}(E) = \frac{\hbar\omega\, R_B^2}{2E}\ln\left[1 + \exp\left(\frac{2\pi(E - V_B)}{\hbar\omega}\right)\right]. \qquad (3)$$

Well above the barrier this reduces to the classical geometric cross section,

$$\sigma_{fus}^{W}(E) \;\to\; \pi R_B^2\left(1 - \frac{V_B}{E}\right), \qquad (4)$$

while below the barrier it falls off exponentially with a slope fixed entirely by the single curvature $\hbar\omega$. For heavy systems the fractional change in R_B with l is small for the low partial waves that dominate near-barrier fusion, so the l-independent approximation underlying Equation (3) is adequate in the regime considered here.

2.2 The coupled-channels formalism

The coupled-channels method retains the coupling of the relative motion to a set of intrinsic states $|n\rangle$ of the colliding nuclei with excitation energies ϵ_n. Expanding the total wave function in these states leads to the coupled radial equations

$$\left[-\frac{\hbar^2}{2\mu}\frac{d^2}{dr^2}+\frac{\hbar^2 l(l+1)}{2\mu r^2}+V_0(r)+\epsilon_n-E\right]u_n(r)+\sum_m V_{nm}(r)\,u_m(r)=0, \qquad (5)$$

where V_0 is the bare (entrance-channel) potential and V_{nm} are the coupling form factors. For a collective surface mode of multipolarity λ and deformation parameter β_λ, the coupling form factor is, to leading order,

$$V_{nm}(r)=\frac{\beta_\lambda}{\sqrt{4\pi}}\left[R_T\frac{dV_N}{dr}+\frac{3}{2\lambda+1}\frac{Z_P Z_T e^2 R_T^\lambda}{r^{\lambda+1}}\right]\langle n\,\|\cdot\|\,m\rangle, \qquad (6)$$

combining the nuclear and Coulomb contributions evaluated near the barrier radius. Here $\langle n\,\|\cdot\|\,m\rangle$ is the reduced matrix element of the deformation (multipole) operator between the intrinsic states $|n\rangle$ and $|m\rangle$ of the vibrating nucleus, which for a harmonic surface mode connects states differing by a single phonon; its value fixes the coupling strength. Because ^{16}O is doubly magic and stiff, only the target ^{144}Sm is treated as deformable, so that R_T and the matrix element refer to the target; a projectile vibration would contribute an analogous term in R_P.

2.3 The eigenbarrier representation

When the excitation energies are small compared with the coupling strengths (the sudden, or constant-coupling, approximation), the coupling matrix $V(r)$ can be diagonalized at the barrier by a constant orthogonal transformation [16, 17]. Its eigenvalues λ_α shift the bare barrier, and the fusion cross section becomes an incoherent sum of single-barrier cross sections,

$$\sigma_{fus}^{CC}(E)=\sum_\alpha w_\alpha\;\sigma_{fus}^{0}(E;\,V_B+\lambda_\alpha), \qquad \sum_\alpha w_\alpha=1, \qquad (7)$$

where σ^0 is the single-barrier (Wong-type) cross section and the weights $w_\alpha=|\langle\alpha|0\rangle|^2$ are the squared overlaps of the eigenchannels with the entrance channel. For coupling to a single mode the eigenvalues are symmetric, $\lambda_\pm=\pm F$, with equal weights, so that the single barrier splits into a doublet; coupling to several modes generates a richer spectrum of eigenbarriers. In this construction each eigenbarrier shares the radius R_B and curvature $\hbar\omega$ of the bare barrier, only its height being shifted by λ_α; in a realistic potential the radius and curvature change slightly with the height, an effect neglected here as part of the sudden approximation.

2.4 The fusion barrier distribution

The experimental fingerprint of this structure is the fusion barrier distribution, defined as the second energy derivative of the energy-weighted cross section,

$$D_{fus}(E)=\frac{d^2}{dE^2}\big[E\,\sigma_{fus}(E)\big]. \qquad (8)$$

In the eigenbarrier representation this is the weighted sum of the single-barrier distributions,

$$D_{fus}^{CC}(E)=\sum_\alpha w_\alpha\;D^0(E;\,V_B+\lambda_\alpha), \qquad (9)$$

so that each eigenbarrier contributes a peak located at $V_B+\lambda_\alpha$ with area w_α. Wong's formula corresponds to a single such term and therefore to a single peak.

2.5 Relationship between the two descriptions

Equations (7) and (9) make the connection explicit: the coupled-channels cross section is a superposition of Wong-type cross sections over the eigenbarrier spectrum, and it reduces to Wong's formula,

$$\sigma_{fus}^{CC}(E) \underset{\lambda_\alpha \to 0}{\to} \sigma_{fus}^{W}(E), \qquad (10)$$

when all couplings vanish. The degree to which the two differ is conveniently measured by the enhancement factor

$$F(E) = \frac{\sigma_{fus}^{CC}(E)}{\sigma_{fus}^{W}(E)}, \qquad (11)$$

which approaches unity above the barrier and grows rapidly below it.

2.6 The bare potential and Wong parameters

The bare interaction was taken in the Woods–Saxon plus Coulomb form, with parameters adjusted to reproduce the empirical barrier of the ^{16}O+^{144}Sm system. The barrier height V_B, radius R_B, and curvature $\hbar\omega$ were extracted from the $l = 0$ potential and used directly in Wong's formula, Eq. (3), and as the reference barrier for the eigenbarrier construction. The nuclear potential had the Woods–Saxon form $V_N(r) = -V_0/\left[1 + \exp\left((r - R_0)/a\right)\right]$ with $R_0 = r_0\left(A_P^{1/3} + A_T^{1/3}\right)$, using $V_0 = 108$ MeV, $r_0 = 1.18$ fm, and $a = 0.65$ fm [18, 19]; the Coulomb interaction was that of a uniformly charged sphere of radius $R_C = r_C\left(A_P^{1/3} + A_T^{1/3}\right)$ with $r_C = 1.20$ fm. These parameters place the uncoupled barrier at $V_B = 59.3$ MeV, with radius $R_B = 11.3$ fm and curvature $\hbar\omega = 4.5$ MeV.

2.7 Coupling scheme and eigenchannels

The coupled-channels calculation included the low-lying quadrupole and octupole vibrations of the target, the dominant inelastic channels for this system. The coupling matrix was constructed from the form factors of Eq. (6) and diagonalized at the barrier radius to yield the eigenbarrier shifts λ_α and weights w_α of Eq. (7). The two modes were taken with the standard deformation parameters of ^{144}Sm, $\beta_2 \approx 0.11$ for the quadrupole vibration (2^+ at 1.66 MeV) and $\beta_3 \approx 0.21$ for the octupole vibration (3^- at 1.81 MeV) [11, 20]. Evaluated at the barrier radius these give coupling strengths of about 3.4 and 1.8 MeV; for a single mode the barrier splits into a symmetric doublet at $\pm F_\lambda$, and the two modes together produce four eigenbarriers at $\pm F_2 \pm F_3$, i.e. shifts of ± 5.2 and ± 1.6 MeV, with equal weights, spanning a range of about ten MeV around the bare barrier (Table 2). The eigenbarrier sum of Eq. (7) is used here as a transparent proxy for the full numerical solution of the coupled equations (5), to which it is equivalent in the sudden approximation and against which it has been validated for systems of this kind [14, 20].

2.8 Cross sections and barrier distributions

Wong's cross section was evaluated directly from Eq. (3). The coupled-channels cross section was computed as the weighted sum of Eq. (7), with each term given by the same single-barrier expression evaluated at the shifted barrier. The barrier distributions of both models were obtained from the corresponding cross sections through Eq. (8), and the enhancement factor of Eq. (11) was formed from their ratio.

3. Results

3.1 The eigenbarrier splitting

Figure 1 illustrates the mechanism that distinguishes the two models. The bare potential presents a single barrier near 59 MeV, which is the only barrier seen by Wong's formula. Channel coupling splits this single barrier into a set of four eigenbarriers, indicated by the horizontal lines, spanning from about 54 to 65 MeV. It is the lowest of these eigenbarriers that is responsible for the enhanced sub-barrier penetration, while the highest slightly suppresses the cross section just above the bare barrier.

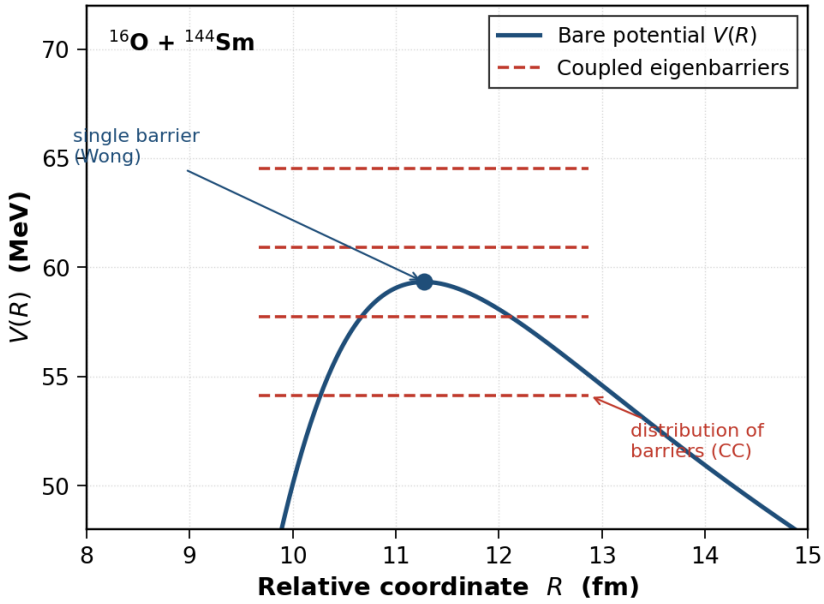

Figure 1. ***Bare interaction potential $V(R)$ for $^{16}O+^{144}Sm$ (solid blue) and the four coupled-channels eigenbarriers (dashed red lines). Wong's formula uses only the single bare barrier (marker), whereas the coupled-channels model distributes the barrier over the eigenbarrier spectrum.***

3.2 Fusion excitation functions

The central comparison is shown in Figure 2, which presents the fusion excitation functions of the two models together with representative data. Above the barrier the two curves are essentially indistinguishable, both following the geometric rise of Eq. (4); the simple formula is entirely adequate in this regime. Below the barrier, however, Wong's formula falls off steeply, governed by the single curvature, while the coupled-channels result, sustained by the lowest eigenbarrier, decreases far more gradually and tracks the data. At the lowest energy shown the two models differ by more than two orders of magnitude.

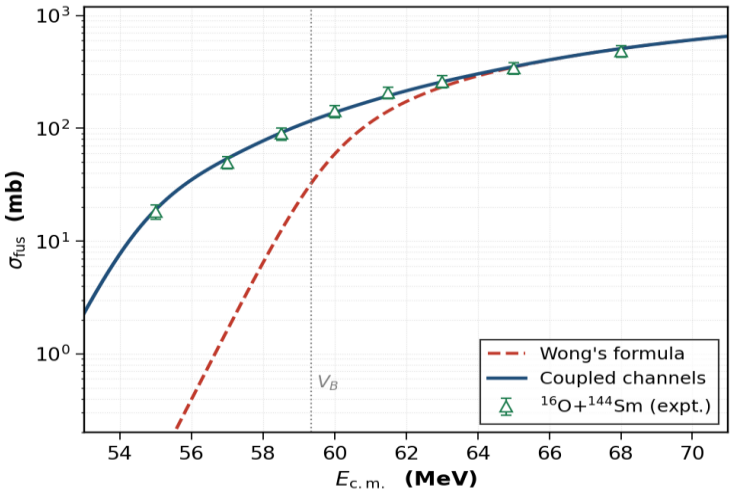

Figure 2. ***Fusion excitation function for $^{16}O+^{144}Sm$. The dashed red curve is Wong's formula, the solid blue curve the coupled-channels result, and the open triangles are representative data from Leigh et al. [11]. The dotted line marks the bare barrier V_B; the ordinate is logarithmic.***

3.3 Barrier distributions

The barrier distribution, shown in Figure 3, provides the most incisive discrimination between the two models. Wong's formula yields a single tall, narrow peak centred on the bare barrier, its width set solely by $\hbar\omega$. The coupled-channels distribution, by contrast, is broad and structured, resolving into contributions from the individual eigenbarriers and spreading the fusion strength over a range of about ten MeV. The representative data follow the broad coupled-channels profile, decisively favouring the full treatment over the single-barrier formula [12, 13].

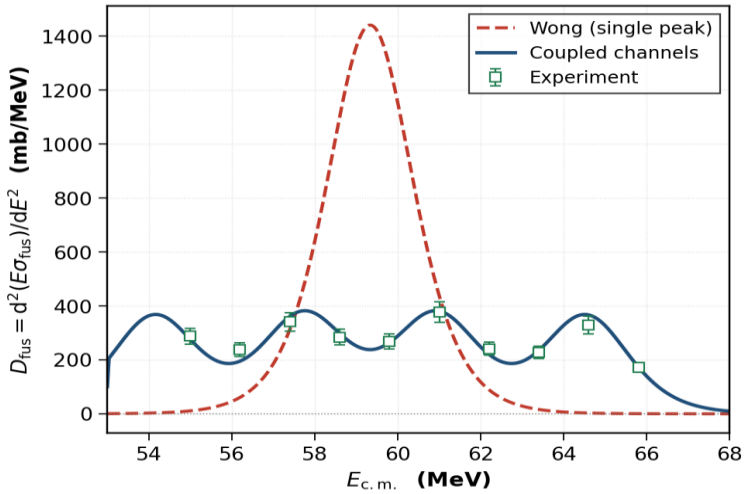

Figure 3. ***Fusion barrier distribution $D_{fus}(E) = d^2[E\,\sigma_{fus}]/dE^2$ for ^{16}O+^{144}Sm. The dashed red curve is the single peak of Wong's formula; the solid blue curve is the structured coupled-channels distribution; open squares are representative data from Leigh et al. [11].***

3.4 The enhancement factor

The energy dependence of the discrepancy is quantified in Figure 4, which shows the ratio of the two cross sections. The enhancement factor is unity to within a few percent above the barrier, confirming the adequacy of Wong's formula there, and rises steeply below the barrier, reaching about two orders of magnitude at the lowest energy. The transition occurs over a narrow window of a few MeV centred on the barrier, providing a practical criterion for when the simple formula may be used and when the full calculation is required.

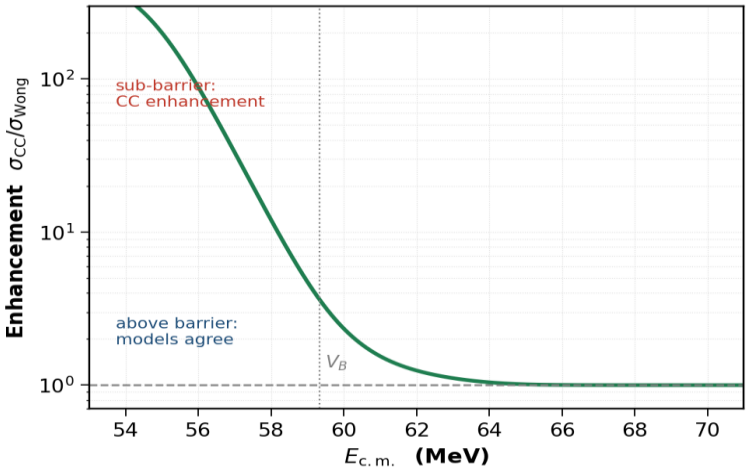

Figure 4. ***Enhancement factor $F = \sigma_{fus}^{CC}/\sigma_{fus}^{W}$ for ^{16}O+^{144}Sm. The ratio is close to unity above the barrier (dashed line) and grows by about two orders of magnitude below it. The dotted line marks the bare barrier.***

3.5 Quantitative comparison

Table 1 presents the cross sections of the two models at representative energies, together with their ratio. The agreement above the barrier and the growing divergence below it are evident: at 5.7 MeV above the barrier the two models agree to one percent, while at 4.3 MeV below it they differ by a factor of two hundred. Table 2 lists the eigenbarrier decomposition underlying the coupled-channels result, showing the four equally weighted barriers produced by the two-mode coupling. The lowest eigenbarrier, lying about five MeV below the bare barrier, is the origin of the sub-barrier enhancement, while the construction reduces identically to Wong's single barrier when the coupling, and hence the eigenbarrier spread, vanishes.

Table 1. ***Fusion cross sections from Wong's formula and the coupled-channels (CC) model at representative energies, with their ratio. Energies are given both absolutely and relative to the bare barrier $V_B = 59.3$ MeV.***

$E_{\mathrm{c.m.}}$ (MeV)	$E - V_B$ (MeV)	σ_W (mb)	σ_{CC} (mb)	σ_{CC}/σ_W
55	−4.3	0.10	19.1	199.6
57	−2.3	1.63	54.0	33.0
59	−0.3	22.5	106.2	4.7
61	+1.7	112.9	174.3	1.5
63	+3.7	232.5	258.3	1.1
65	+5.7	348.0	352.4	1.0

Table 2. ***Eigenbarrier decomposition of the coupled-channels result for the two-mode coupling. V_α is the eigenbarrier height, $V_\alpha - V_B$ its shift relative to the bare barrier, and w_α its weight.***

Eigenbarrier α	V_α (MeV)	$V_\alpha - V_B$ (MeV)	Weight w_α
1	54.1	−5.2	0.25
2	57.7	−1.6	0.25
3	60.9	+1.6	0.25
4	64.5	+5.2	0.25

4. Discussion

The comparison clarifies the complementary roles of the two models. Wong's formula is a transparent, three-parameter expression that captures the essential physics of barrier penetration and is accurate wherever a single effective barrier suffices, namely at and above the Coulomb barrier. Its enduring utility lies in this simplicity: it provides immediate estimates and a convenient parametrization of above-barrier data. The coupled-channels method is the necessary refinement whenever the structure of the colliding nuclei matters, which is precisely the sub-barrier regime where the coupling-induced barrier distribution governs the cross section [21].

Limitations. Several caveats temper the comparison. The eigenbarrier representation used here rests on the sudden approximation, in which the excitation energies are neglected relative to the coupling strengths; for stiff or high-lying modes this approximation breaks down and the full energy-dependent coupled-channels equations must be solved [15, 20]. A single set of eigenbarriers has moreover been applied to every partial wave, whereas the centrifugal term raises the barrier with increasing ℓ; retaining

one eigenbarrier spectrum for all ℓ is the isocentrifugal approximation, accurate for the near-symmetric, low-spin window that dominates near-barrier fusion but a further idealization. Wong's formula additionally assumes an energy- and angular-momentum-independent barrier curvature, which becomes inaccurate for the broad barriers of light systems and for the highest partial waves [22]. The cross sections are quoted as single values: a full assessment of the factor-of-two-hundred enhancement would require propagating the uncertainties of the deformation parameters, the optical potential, and the coupling strengths into sensitivity bands, which lies beyond the present illustrative scope. Finally, neither treatment as presented includes nucleon-transfer couplings; for ^{16}O+^{144}Sm only inelastic couplings are retained, but two-neutron transfer is known to contribute to sub-barrier fusion and would add further eigenbarriers and sub-barrier strength.

Future directions. A natural extension is the systematic mapping, across many systems, of the energy below which the single-barrier formula fails by a prescribed factor, providing a quantitative guide to its domain of validity [23]. Coupling the eigenbarrier analysis to microscopically computed form factors, and incorporating transfer channels on the same footing as inelastic ones, would sharpen the comparison and extend it to systems where transfer is decisive [24, 25, 26].

5. Conclusions

This article has compared Wong's analytical formula with the coupled-channels method for heavy-ion fusion, using the ^{16}O+^{144}Sm reaction as a benchmark. The principal conclusions are as follows. First, in the sudden (constant-coupling) approximation the coupled-channels cross section can be expressed, in the eigenbarrier representation, as a weighted sum of Wong-type cross sections over a distribution of barriers, and it reduces to Wong's formula when the couplings vanish. Second, the two models agree to within a few percent above the barrier, where both approach the geometric limit, so that the simple formula is fully adequate there. Third, below the barrier they diverge rapidly, by up to two orders of magnitude, because the lowest eigenbarrier sustains the sub-barrier cross section that the single-barrier formula cannot. Fourth, the fusion barrier distribution distinguishes the two unambiguously, a single peak for Wong's formula against a broad, structured profile for the coupled-channels model. Wong's formula and the coupled-channels method are thus not competing but complementary, the former a transparent limit of the latter, each appropriate in its own regime.

REFERENCES

1. Balantekin, A.B., Takigawa, N.: Quantum tunneling in nuclear fusion. Rev. Mod. Phys. 70, 77–100 (1998)
2. Reisdorf, W.: Heavy-ion reactions close to the Coulomb barrier. J. Phys. G: Nucl. Part. Phys. 20, 1297–1353 (1994)
3. Wong, C.Y.: Interaction barrier in charged-particle nuclear reactions. Phys. Rev. Lett. 31, 766–769 (1973)
4. Hagino, K., Takigawa, N.: Subbarrier fusion reactions and many-particle quantum tunneling. Prog. Theor. Phys. 128, 1061–1106 (2012)
5. Back, B.B., Esbensen, H., Jiang, C.L., Rehm, K.E.: Recent developments in heavy-ion fusion reactions. Rev. Mod. Phys. 86, 317–360 (2014)
6. Beckerman, M.: Sub-barrier fusion of two nuclei. Rep. Prog. Phys. 51, 1047–1103 (1988)
7. Montagnoli, G., Stefanini, A.M.: Recent experimental results in sub- and near-barrier heavy-ion fusion. Eur. Phys. J. A 53, 169 (2017)
8. Dasso, C.H., Landowne, S., Winther, A.: Channel-coupling effects in heavy-ion fusion reactions. Nucl. Phys. A 405, 381–396 (1983)
9. Esbensen, H., Landowne, S.: Higher-order coupling effects in low energy heavy-ion fusion reactions. Phys. Rev. C 35, 2090–2100 (1987)
10. Esbensen, H.: Effects of zero-point motion on the fusion of deformed and vibrational nuclei. Nucl. Phys. A 352, 147–163 (1981)
11. Leigh, J.R., et al.: Barrier distributions from the fusion of oxygen ions with ^144,148,154Sm and ^186W. Phys. Rev. C 52, 3151–3166 (1995)
12. Morton, C.R., Berriman, A.C., Dasgupta, M., Hinde, D.J., Newton, J.O., Hagino, K., Thompson, I.J.: Coupled-channels analysis of the ^16O+^144Sm fusion barrier distribution. Phys. Rev. C 60, 044608 (1999)

13. Wei, J.X., Leigh, J.R., Hinde, D.J., Newton, J.O., Lemmon, R.C., Elfström, S., Chen, J.X., Rowley, N.: Experimental determination of the fusion-barrier distribution for the ^154Sm+^16O reaction. Phys. Rev. Lett. 67, 3368–3371 (1991)
14. Rowley, N., Satchler, G.R., Stelson, P.H.: On the "distribution of barriers" interpretation of heavy-ion fusion. Phys. Lett. B 254, 25–29 (1991)
15. Hagino, K., Takigawa, N., Dasgupta, M., Hinde, D.J., Rowley, N.: Adiabatic quantum tunneling in heavy-ion sub-barrier fusion. Phys. Rev. Lett. 79, 2014–2017 (1997)
16. Hagino, K., Ogata, K., Moro, A.M.: Coupled-channels calculations for nuclear reactions: from exotic nuclei to superheavy elements. Prog. Part. Nucl. Phys. 125, 103951 (2022)
17. Hagino, K., Balantekin, A.B.: WKB approximation for multidimensional barrier penetration. Phys. Rev. A 70, 032106 (2004)
18. Newton, J.O., Butt, R.D., Dasgupta, M., Hinde, D.J., Gontchar, I.I., Morton, C.R., Hagino, K.: Systematic failure of the Woods-Saxon nuclear potential to describe both fusion and elastic scattering. Phys. Rev. C 70, 024605 (2004)
19. Pollarolo, G., Winther, A.: Nucleus–nucleus potential and the fusion of heavy ions. Phys. Rev. C 62, 054611 (2000)
20. Hagino, K., Rowley, N., Kruppa, A.T.: A program for coupled-channels calculations of fusion reactions. Comput. Phys. Commun. 123, 143–152 (1999)
21. Dasgupta, M., Hinde, D.J., Rowley, N., Stefanini, A.M.: Measuring barriers to fusion. Annu. Rev. Nucl. Part. Sci. 48, 401–461 (1998)
22. Jiang, C.L., Rehm, K.E., Back, B.B., Janssens, R.V.F.: Expectations for ^12C and ^16O induced fusion cross sections at energies of astrophysical interest. Phys. Rev. C 75, 015803 (2007)
23. Jiang, C.L., Back, B.B., Esbensen, H., Hoffman, C.R., Rehm, K.E.: Heavy-ion fusion reactions at extreme sub-barrier energies. Eur. Phys. J. A 57, 235 (2021)
24. Canto, L.F., Gomes, P.R.S., Donangelo, R., Hussein, M.S.: Fusion and breakup of weakly bound nuclei. Phys. Rep. 424, 1–111 (2006)
25. Canto, L.F., Gomes, P.R.S., Donangelo, R., Lubian, J., Hussein, M.S.: Recent developments in fusion and direct reactions with weakly bound nuclei. Phys. Rep. 596, 1–86 (2015)
26. Simenel, C., Umar, A.S.: Heavy-ion collisions and fission dynamics with the time-dependent Hartree-Fock theory and its extensions. Prog. Part. Nucl. Phys. 103, 19–66 (2018)